Cerebellum (2014) 13:580–587
DOI 10.1007/s12311-014-0575-2

ORIGINAL PAPER

Quantitative Longitudinal Evaluation of Diaschisis-Related Cerebellar Perfusion and Diffusion Parameters in Patients with Supratentorial Hemispheric High-Grade Gliomas After Surgery

Zoltan Patay · Carlos Parra · Harris Hawk · Arun George · Yimei Li · Matthew Scoggins · Alberto Broniscer · Robert J. Ogg

Published online: 12 June 2014

Abstract Decreased cerebral blood volume (CBV) in contralateral cerebellar gray matter (cGM) in conjunction with cerebellar white matter (cWM) damage, consistent with crossed cerebro-cerebellar diaschisis (cCCD) develop following supratentorial hemispheric stroke. In this study, we investigated the longitudinal evolution of diaschisis-related cerebellar perfusion and diffusion tensor-imaging (DTI) changes in patients after surgery for supratentorial brain tumors. Eight patients (M:F 5:3, age 8–22 years) who received surgery for supratentorial high-grade gliomas were evaluated. Initial MRI studies were performed 19–54 days postoperatively, with follow-ups at 2- to 3-month intervals. For each study, parametric maps of the cerebellum were generated and coregistered to T1-weighted images that had been previously segmented for cGM and cWM. Aggregate mean values of CBV, cerebral blood flow (CBF), and fractional anisotropy (FA) were obtained separately for cGM and cWM, and asymmetry indices (AIs) were calculated. Hemodynamic changes were more robust in cGM than in cWM. Seven patients showed decreased perfusion within cGM contralateral to the supratentorial lesion on the first postoperative study, and asymmetry was significant for both CBV ($p=0.008$) and CBF ($p<0.01$). For CBV, follow-up studies showed a significant trend towards recovery ($p<0.02$). DTI changes were more pronounced in cWM. FA values suggested a "paradoxical" increase at initial follow-up, but steadily declined thereafter ($p=0.0003$), without evidence of subsequent recovery. Diaschisis-related hemodynamic alterations within cGM appear on early postoperative studies, but CBV recovers over time. Conversely, cWM DTI changes are delayed and progressive. Although the clinical correlates of cCCD are yet to be elucidated, better understanding of longitudinal structural and hemodynamic changes within brain remote from the area of primary insult could have implications in research and clinical rehabilitative strategies.

Keywords Diaschisis · Cerebellar perfusion · Diffusion tensor imaging · Functional connectivity · Magnetic resonance imaging

Z. Patay
Section of Neuroimaging, Department of Radiological Sciences, St. Jude Children's Research Hospital, 262 Danny Thomas Place, Memphis, TN 38105-3678, USA

C. Parra · M. Scoggins · R. J. Ogg
Division of Translational Imaging Research, Department of Radiological Sciences, St. Jude Children's Research Hospital, 262 Danny Thomas Place, Memphis, TN 38105-3678, USA

H. Hawk
Diagnostic Neuroradiology, Department of Radiology, Medical University of South Carolina, MSC 322, 169 Ashley Avenue, Charleston, SC 29425, USA

A. George
Department of Anesthesiology and Critical Care, Padmashree Dr. D. Y. Patil Medical College, Hospital and Research Centre, Pimpri, Pune 411018, India

Y. Li
Department of Biostatistics, St. Jude Children's Research Hospital, 262 Danny Thomas Place, Memphis, TN 38105-3678, USA

A. Broniscer
Division of Neuro-Oncology, Department of Oncology, St. Jude Children's Research Hospital, 262 Danny Thomas Place, Memphis, TN 38105-3678, USA

Z. Patay (✉)
Department of Radiological Sciences, St. Jude Children's Research Hospital, 262 Danny Thomas Place, Mail Stop 220, Memphis, TN 38105-3678, USA
e-mail: zoltan.patay@stjude.org

Introduction

The term diaschisis was introduced by the Russian–Swiss neuropathologist Constantin von Monakow in the early part of the 20th century. He intended the word to describe an insult to the brain: when translated from the Greek derivation, it means "shocked throughout." In modern neuroscience, the term is used to describe an acute, localized, secondary functional disturbance in an area of the brain that is at a distance from, but anatomically connected to, another site of primary brain injury through fiber tracts. The most studied form of diaschisis is the so-called crossed cerebro-cerebellar diaschisis (cCCD), which is presumed to be due to the disruption of the cerebro-ponto-cerebellar neuronal fibers (i.e., the afferent cerebellar pathway). cCCD has been widely investigated and primarily described in the nuclear medicine literature on the basis of decreased glucose use and blood flow. In ^{18}FDG positron emission tomography (PET) studies, cCCD is indicated by glucose hypometabolism in the affected cerebellar hemisphere contralateral to a supratentorial insult, primarily within the frontoparietal lobes [1]. Single-photon emission computerized tomography (SPECT) examinations using cerebral perfusion agents [hexamethylpropyleneamineoxine (HMPAO) and ethyl cysteinate dimer (ECD)] show hypoperfusion in the same pattern [2, 3]. More recent studies using advanced magnetic resonance imaging (MRI) techniques have revealed measurable drops in perfusion in the cerebellar cortical grey matter (cGM) and evidence of cerebellar white matter (cWM) damage by fractional anisotropy (FA) in cCCD [4–6]. Consequently, MRI-based perfusion and diffusion parameters, such as cerebral blood volume (CBV), cerebral blood flow (CBF), and fractional anisotropy (FA), appear to be reliable and reproducible markers of diaschisis-induced cerebellar parenchymal changes.

To the best of our knowledge, no MRI-based data about the dynamics of these alterations are available. Therefore, we investigated the longitudinal evolution of cGM blood perfusion and cWM integrity changes using dynamic susceptibility contrast (DSC) perfusion MRI and diffusion tensor imaging (DTI) to improve our understanding of the dynamics of the underlying pathophysiologic processes in cCCD.

Patients and Methods

Patient Enrolment

All patients had supratentorial hemispheric high-grade gliomas and were initially treated with surgery resulting in gross total, near-total, or subtotal tumor resection. Subsequently, after written consent, they were enrolled in a prospective clinical trial. The primary research objectives of the trial were the following: (a) to determine the maximum tolerated dose (MTD) and dose-limiting toxicities (DLTs) of an epidermal growth factor receptor (EGFR) inhibitor (Tarceva™, erlotinib hydrochloride) when given during and after radiotherapy to treat children, adolescents, or young adults with newly diagnosed high-grade glioma or unfavorable low-grade glioma; and (b) to estimate the progression-free survival of those receiving this therapy. Although the data used for our retrospective research originated from a prospectively designed trial approved by the Institutional Review Board (IRB), a separate IRB approval and waiver of consent was obtained to allow us to evaluate the MRI data of 8 patients that we used to characterize cCCD (Table 1).

Study Plan

Patients received escalating doses of erlotinib hydrochloride in conjunction with conformal radiation therapy [7]. The starting dose of erlotinib was 70 mg/m^2 (80 % of the MTD in adults), and the dosage was increased at increments of approximately 30 % in cohorts of 3 to 6 patients, following the traditional Phase I study design. Conformal three-dimensional (3D) radiation therapy was given in 1.8 Gy fractions over a period of 6 1/2 weeks for a total cumulative dose of 59.4 Gy. The clinical trial required regular MRI including conventional anatomic imaging, DSC perfusion MRI, and DTI sequences. The first postoperative MRI studies were performed 19–54 days after surgery. Further follow-ups (up to 8/patient) were done at 2- to 3-month intervals. As per protocol requirements, all studies were performed on a 1.5 T MRI scanner (Avanto TIM, Siemens Medical Solutions, Erlangen, Germany) with a circular polarized head coil.

Anatomic Data Collection and Evaluation

Conventional anatomical MRI of the brain included sagittal and axial T1-weighted gradient echo, axial T2-weighted fast spin echo, contrast-enhanced axial fluid-attenuated inversion recovery (FLAIR), axial, coronal T1-weighted gradient echo, and sagittal 3D T1-weighted gradient echo [3D magnetization-prepared rapid acquisition with gradient echo (MP-RAGE)] sequences. These images were evaluated to assess the primary lesion site (the extent of lesion involvement and surgical resection, the presence of residual/recurrent tumor, and the extent of collateral surgical damage) and possible gross morphologic changes of the cerebellum. Using axial FLAIR images, we visually estimated the extent of surgical and tumoral damages as a percentage of the ipsilateral cerebral hemisphere.

Perfusion Data Collection

DSC perfusion MR data were acquired during bolus intravenous injection of a gadolinium-based contrast agent (GBCA),

Table 1 Demographic, histologic, and surgical treatment data

Patient	Gender	Age at diagnosis (years)	Histologic diagnosis (grade)	Location of tumor and surgical involvement	Estimated volume of hemispheric damage (percent)
1	F	8	Glioblastoma multiforme (WHO IV)	Left thalamus and temporal/occipital	25
2	F	14	Glioblastoma multiforme (WHO IV)	Left temporal	30
3	M	23	Anaplastic oligoastrocytoma (WHO III)	Left temporal and insula	15
4	F	18	Anaplastic astrocytoma (WHO III)	Right anterior temporal	15
5	M	12	Anaplastic ganglioglioma (WHO III)	Right frontotemporal and insula	15
6	M	13	Glioblastoma multiforme (WHO IV)	Right temporal	20
7	M	3	Anaplastic oligoastrocytoma (WHO III)	Left posterior frontal	10
8	M	19	Anaplastic astrocytoma (WHO III)	Left frontal	30

at a rate of 0.8 to 1.0 ml/s (n.b., these injection rates were imposed by institutional policy/protocol requirements), through a 22 G intravenous line. The injection was delivered by a power injector, with total injection times being 2 to 13 s. We used the regular dose, 0.1 mmol/kg (0.2 ml/kg); therefore, the total amount of the injected GBCA was a function of the patient's body weight. The DSC sequence used in our patients was an echo-planar-based [free induction decay-echo planar imaging (FID-EPI)] multi-slice two-dimensional (2D) acquisition [TR/TE = 1,910 ms/50 ms, Nex 1, bandwidth 1,346/pixel, field of view (FOV) 210 mm, matrix size of 128×128 with a partial Fourier factor of 7/8, 15 slices, 5-mm slice thickness with no slice gap, and number of measurements per slice 50]. The data acquisition started approximately 35–40 s before the contrast arrived at the intracranial space and ended after a few recirculation passes of contrast, with the first pass being roughly in the middle of the acquisition. Because our technique did not allow for coverage of the entire brain, positioning of the acquisition slab was guided by the location of the supratentorial lesions. This method resulted in varying degrees of coverage of the posterior fossa: it was complete in some cases (e.g., temporal lobe tumors), and it was partial in others (e.g., higher parietal or frontal lesions), encompassing only upper portions of the cerebellum.

DTI Data Collection

DTI was performed by using a twice-refocused spin echo (TRSE)-EPI-DTI sequence [8] having the following parameters: 6 or 12 (after a license upgrade) diffusion-encoding directions with a b value of 1,000 s/mm^2 and 1 image with b=0; TR/TE = 10,000/100 ms; matrix 128×128, FOV= 230×230 mm corresponding to a voxel size of 1.8×1.8 mm; gap between slices=3 mm, NEX=4, 15 slices, 5-mm slice thickness. Bipolar diffusion-encoding gradients were used to reduce gradient-induced eddy currents that cause image distortion and degradation [9]. DTI data were always collected from the whole brain.

Perfusion and DTI Data Analysis

For each patient, the first post-surgical, high-resolution, T1 three-dimensional image (0.82×0.82×1.25 mm) was used as the anatomic reference to which all DTI and perfusion data (including derived maps) were registered (SPM2, Wellcome Institute of Neurology, London, UK, http://www.fil.ion.ucl.ac.uk/spm). Correct registration of all parametric maps associated with each time point was visually verified. Segmentation of the whole brain was performed with the standard Gaussian mixture model method that is part of the statistical parametric mapping (SPM) package [10]. The SPM segmentation procedure was applied to the 3D T1-weighted image for each examination, yielding tissue-class probability maps for gray matter, white matter, and cerebrospinal fluid. Binary gray matter and white matter masks were created by thresholding for tissue-class probability ≥0.8. The perimeters of the left and right cerebellar hemispheres were manually delineated in each slice of the T1 volume to define regions of interest for evaluation of diaschisis-related asymmetry of the perfusion and diffusion parameters (ImageJ, U. S. National Institutes of Health, Bethesda, MD; http://rsbweb.nih.gov/ij/).

CBF and CBV parametric maps were computed by using a proprietary software suite including a "perfusion-weighted imaging" toolbox that was installed on a dedicated multimodality workstation (Siemens Medical Solutions, Erlangen, Germany). DTI data were processed by using the Diffusion II toolbox [extension to SPM (http://www.fil.ion.ucl.ac.uk/spm/ext/#Diffusion_II)]. Grayscale maps for FA, radial diffusivity (RD), and axial diffusivity (AD) were computed after correcting the time series for motion, reorienting gradients accordingly, computing the tensor regression, and then computing the tensor decomposition. The affine registration parameters to register the FA, RD, AD images to the 3D T1 image were computed from the standard SPM mutual information-based registration of the respective b=0 image to the T1 reference. After the parametric maps of CBF, CBV, FA, RD, and AD were registered to the T1 reference images of each patient, cGM and cWM parameters were evaluated

within each cerebellar hemisphere after masking with the binary segmentation of the cerebellar tissues of interest (Fig. 1).

The mean parameters were calculated at each time-point within each tissue segment (i.e., GM, WM) for each cerebellar hemisphere (ipsi-lateral and contra-lateral to the supratentorial tumor). An asymmetry index (AI) was calculated as follows:

$$\mathrm{AI}_{\mathrm{parameter,tissue}} = \frac{\mathrm{parameter}_{\mathrm{tissue,contralateral}} - \mathrm{parameter}_{\mathrm{tissue,ipsilateral}}}{\mathrm{parameter}_{\mathrm{tissue,contralateral}} + \mathrm{parameter}_{\mathrm{tissue,ipsilateral}}}$$

The AI was evaluated longitudinally at nine time points, with the time measured from surgical resection. A linear mixed-effects model was used to characterize the temporal evolution of the asymmetry indices in the cerebellum. The model included fixed effects (i.e., intercepts and slopes) for each parameter–tissue combination (e.g., CBV in GM and CBV in WM) and nested random effects (intercepts) for each parameter (CBF, CBV, and FA) within each tissue type (GM and WM) within each patient. As described earlier, the coverage of the cerebellum in the images was variable because the primary target for the protocol-based imaging was the supratentorial tumor. The total number of image voxels contributing to each AI was entered into a linear mixed-effects model to test the influence of image coverage on the measured asymmetry. In a separate analysis, linear models were used to characterize the relationship of FA to RD and AD. Statistical analyses were performed with R, using the *lme* function for mixed-effects models [7].

Results

Anatomic Evaluation

No perceptible morphologic changes or signal alterations in the cerebellum were found to develop in any of our patients within the study interval. We did not volumetrically evaluate the supratentorial lesion burden (defined as the sum of the volumes of the surgical resection cavity and the residual tumor), but we made a visual estimate for each patient (Table 1). In all cases, the actual supratentorial lesion burden was more than 10 % of the volume of the affected cerebral hemisphere (range 10–30 %). The most common lesion location in our series was the temporal and the frontal lobes. Tumors remained limited to one hemisphere in all cases (i.e., no contralateral extension) throughout the evaluation period, even in cases having conventional imaging evidence of tumor progression.

Advanced MRI Evaluation

No significant association existed between AI and the number of voxels evaluated for any of the parameter–tissue combinations. Summary AI data for each measured parameter–tissue versus time since surgery are shown in Fig. 2.

Hemodynamic changes were more robust in cGM than in cWM. During the first postoperative study, 7 patients had decreased blood perfusion within cGM contralateral to supratentorial lesion, and the asymmetry was statistically significant (intercept of the fixed effects regression) for both

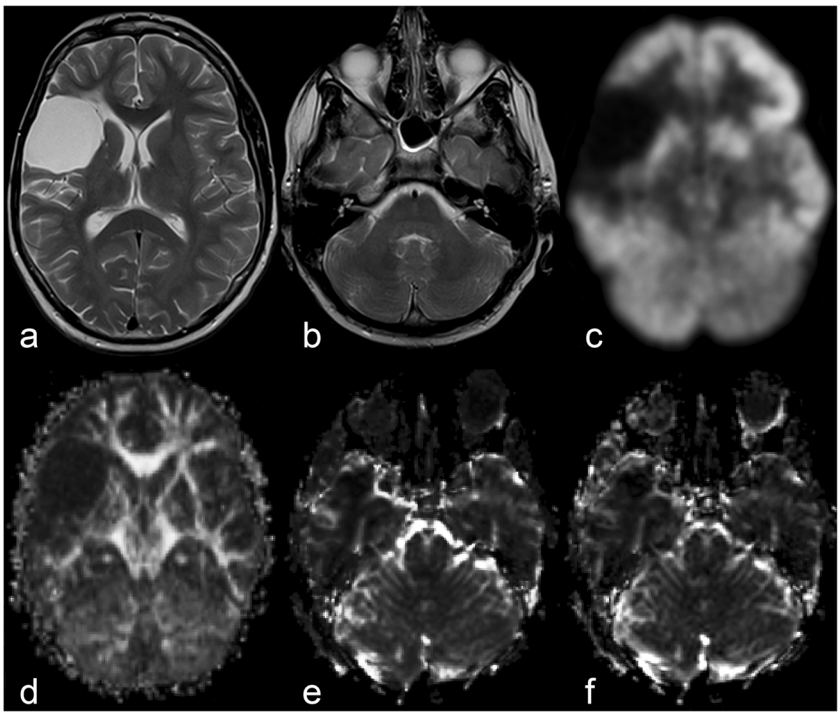

Fig. 1 Post-operative axial T2-weighted images of the supratentorial lesion area (**a**) and cerebellum (**b**). Axial ^{18}FDG PET images of the cerebellum, showing decreased metabolic activity within left cerebellar cortex consistent with diaschisis (**c**). Axial parametric maps of FA (**d**), CBV (**e**), and CBF (**f**). All images are of the same patient (#5)

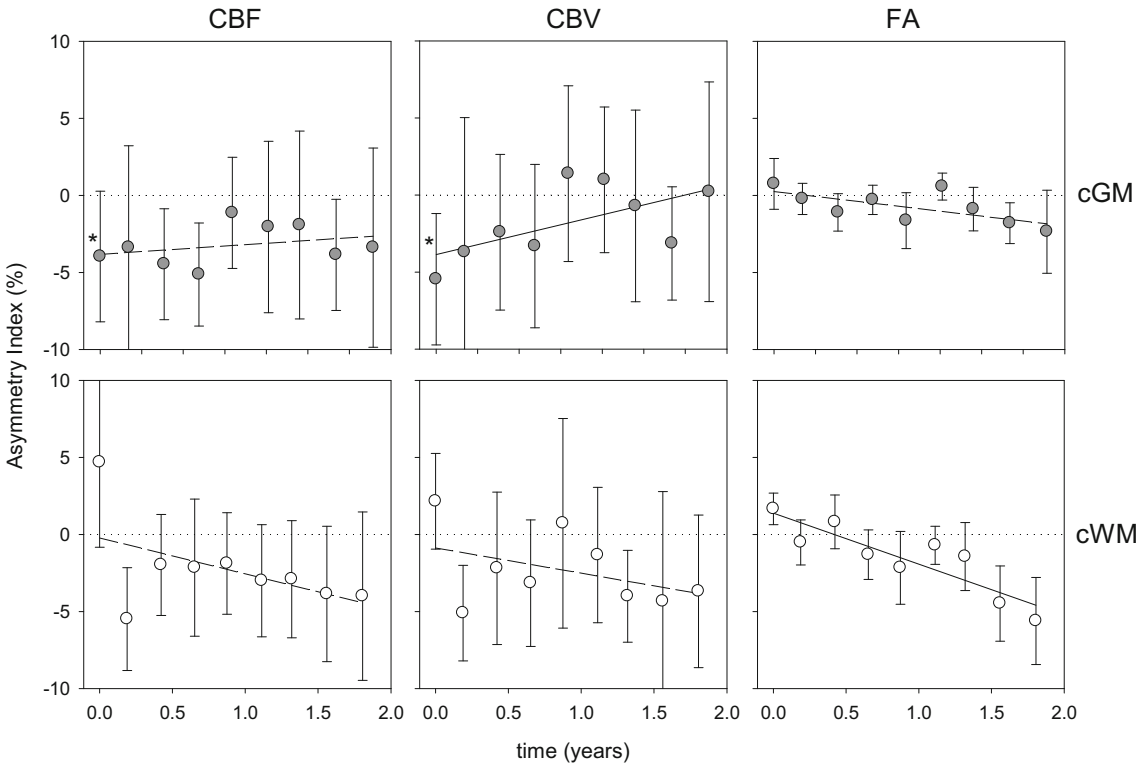

Fig. 2 Asymmetry index for cerebral blood flow (*CBF*), cerebral blood volume (*CBV*), and fractional anisotropy (*FA*) in cerebellar grey matter (*cGM*) and cerebellar white matter (*cWM*). The points represent the mean and standard error of the asymmetry index across patients at each nominal protocol time point. The regression lines represent the fixed effects from the full mixed-effects model. The asterisk (*) indicates a significant, non-zero intercept for CBF and CBV in the gray matter, and solid lines indicate significant slopes for CBV in gray matter and FA in white matter

CBV (p=0.008) and CBF (p<0.01). The asymmetry was in the range of 3–15 % (median 6 %) for CBV and 2–6 % (median 4 %) for CBF. Asymmetry of CBV trended significantly toward recovery (p<0.02), reaching symmetry after 2 years. In contrast, CBF remained asymmetric for the duration of the study. The regression of CBV and CBF in cWM was not significant. The pattern of hemodynamic changes in cWM suggests a paradoxical increase after surgery and a large decrease at first follow-up, perhaps representing a delayed response in the white matter compared to the more metabolically active gray matter.

DTI changes were more pronounced in cWM than in cGM. The FA in contralateral cWM steadily declined (p=0.003), without evidence of recovery during the follow-up period. FA in cGM followed a similar trend; however, the slope was not statistically significant. The decline in cWM FA contralateral to the supratentorial lesion was associated with an increase in radial diffusivity (p=0.04), with no systematic change in the axial diffusivity (Fig. 3).

Discussion

Crossed cerebro-cerebellar diaschisis is a powerful example of the well-known interdependency of interconnected yet remote areas of the brain. Because the pathophysiological sequelae of diaschisis are most likely due to the loss of structural integrity at one level of a functional system (neuron populations interconnected by white matter bundles through one or more synaptic relays), the resultant disconnection between these functionally interdependent structures leads to functional and structural degradation of a seemingly unaffected, remote region. It is, therefore, logical to presume that diaschisis is a universal trans-synaptic response mechanism to brain injury

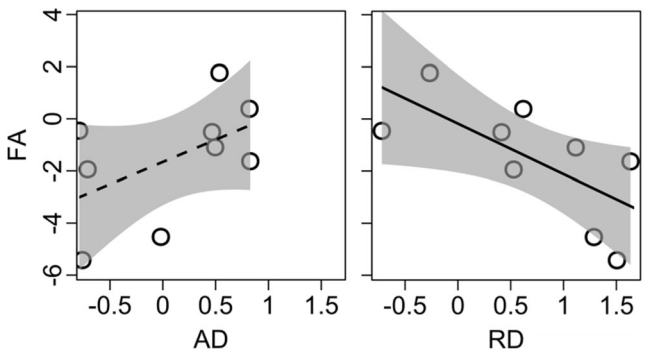

Fig. 3 Asymmetry of fractional anisotropy (*FA*) versus axial diffusivity (*AD*) and radial diffusivity (*RD*) in cerebellar the cerebellar white matter. The FA asymmetry values are the same as shown in Fig. 2, and there was a significant negative correlation between FA and RD. FA was not associated with AD

that may present with more or less significant neurologic or neuropsychologic manifestations, depending on the eloquence of the affected area. Indeed, it was recently suggested that reversed cerebello-cerebral diaschisis is the likely pathomechanism of the so-called postoperative posterior fossa syndrome (PFS). PFS is seen in up to 25 % of pediatric patients undergoing surgical treatment for midline cerebellar tumors, and the central manifestation of this complex condition is cerebellar mutism (a peculiar form of speech apraxia), likely due to diaschisis-related negative perfusion changes in supratentorial cerebral cortex with frontal predominance [11]. Diaschisis should not be confused with Wallerian degeneration, which represents disintegration of the axonal membrane and skeleton as well as secondary breakdown of the axon's myelin sheath distal to an injury to the neuroaxonal unit. However, due to injury to neurons in the primary lesion site, Wallerian degeneration likely also occurs in diaschisis along the first segment of the affected functional system.

Advanced MRI techniques can detect changes in regional brain perfusion and fiber tract integrity [5, 6]. T2*-weighted DSC perfusion MRI has been widely used to evaluate brain perfusion and provides quantitative measurements of parameters such as relative CBF and CBV [12]. Using this technique, investigators have shown perfusion changes (i.e., decreased CBV) within the cerebellar cortex in patients with contralateral cerebral infarctions [6]. DTI is a reliable indicator of white matter integrity and provides parametric information about the structural integrity of myelinated axons in brain parenchyma [13]. DTI has been used to show FA reduction in the contralateral middle cerebellar peduncle, a fairly robust white matter structure, in patients with chronic cerebral hemispheric stroke [5]. These observations suggest that both DSC and DTI may be useable markers of functional (blood perfusion) and structural (myelin integrity) changes in cCCD, respectively, and support the appropriateness of using DSC perfusion MRI and DTI to characterize presumed diaschisis-related changes in brain parenchyma in various settings.

One of the distinctive conventional cross-sectional imaging features in diaschisis is the initial lack of associated morphologic (e.g., atrophy and swelling) or signal/density changes in affected brain structures. Our study validates this observation, with none of our patients having appreciable cerebellar volume loss or signal changes during the study period. However, others have described trophic changes within the affected cerebellar hemisphere late during the course of diaschisis [1].

Most investigators agree that diaschisis-related hemodynamic alterations within cGM are probably immediate, but available data is inconsistent about the onset of these phenomena as detected by DSC perfusion MRI [8, 14]. For instance, such changes in time-to-peak have been seen as early as 5 days after a supratentorial stroke; however, CBV changes were much more reliably seen in the subacute to chronic phase, 6–120 days after the stroke [4]. Interestingly, the clinical manifestations of the aforementioned postoperative PFS also develop a few days after surgical damage to the bilateral proximal efferent cerebellar pathway (dentate nuclei, superior cerebellar peduncles). Again, the reason for this short, latent period is unknown.

The magnitude of cCCD is likely related to the extent of the supratentorial destructive process. One may also speculate that the contribution of different cortical areas to the afferent cerebellar signaling may not be identical either; frontal–parietal regions may have the most significant input because of their known contribution to the afferent cerebellar pathway. Therefore, damage to these areas should lead to more robust diaschisis-related functional changes, but in our series, lesions primarily involving the temporal lobe produced measurable diaschisis-related changes in the cerebellum too.

Unfortunately, only limited clinically detectable sequelae to cCCD have been identified and described; therefore, the timing of the onset of a possible associated "clinical syndrome" is difficult to determine. In supratentorial subcortical lacunar syndromes, the secondary, more subtle diaschisis-related cerebellar symptoms may be "unmasked" due to the lack of direct cortical damage. For example, small "well-placed" infarcts in the subcortical white matter are associated with contralateral ataxic hemiparesis, suggesting cerebellar involvement in the resultant neurologic deficit [15, 16] These symptoms seemed to improve over time, with the prognosis of recovery related to the degree of underlying cerebellar dysfunction (i.e., hypoperfusion and hypometabolism) measured during the subacute phase [17].

We believe that one of the most important proceedings of our study may be that our data suggests that perfusion changes in cCCD recover over time. It seems that CBV, but not CBF, in cGM may normalize to baseline asymmetry (i.e., gross physiological symmetry) after approximately 2 years. Further studies are needed to determine whether CBF ever truly normalizes. If it does not, one explanation may be that fractional blood volume equilibrates to a new steady state over time, but the actual flow remains decreased, consistent with the persistently diminished local metabolic demand.

Our data show that changes within cWM do occur, but are slower than cGM changes and are apparently progressive on all accounts. Both CBV and CBF in the white matter increase rapidly after surgery, but subsequently decline and do not recover again. Loss of FA caused by increased radial diffusivity in cWM is also delayed, but may also be preceded by a mild initial increase. Again, one may only speculate about the underlying histopathologic and pathophysiologic processes causing this. It is possible that an abrupt drop of cerebral input and relative inactivity of afferent cerebellar fiber tracts initially lead to swelling of degenerating myelin sheaths, with resultant retraction of extracellular space. Hence, FA may increase transiently, followed by myelin loss and/or tissue rarefaction that lead to RD increase and FA decrease.

It is increasingly evident that myelination is driven by both genetic factors and function in the developing brain [18]. It is conceivable too that appropriate myelin maintenance is dependent on sustained utilization of the fiber tracts. In diaschisis, specific neural networks become underutilized, which may manifest with decreased metabolism and blood perfusion as well as myelin "degeneration" in the affected regions. Our DTI data analysis is concordant with this; in that FA changes in the cerebellar white matter in cerebro-cerebellar diaschisis are driven by increased radial diffusivity, which is a known surrogate marker of the "quality" of myelin, suggesting therefore a slow degradation without complete breakdown of myelin in response to chronic diminished utilization.

The reason for the early increase of CBV and CBF in cWM is unclear. The delay of the onset of negative perfusion changes within cWM versus those of cGM may reflect the relatively lower and less dynamic baseline metabolic needs of cWM compared to cGM. The prolonged and possibly permanent asymmetry of white matter perfusion may represent the hemodynamic correlates of the irreversible degenerative changes indicated by declining anisotropy of water diffusion.

A new, powerful technique in advanced MRI, called resting-state functional MRI, appears poised to elucidate functional brain connectivity and is a prognostic indicator after stroke [19]. This technique can identify regions of remote functional connectivity that, when disrupted or activated after brain injury, can either highlight remote functional sequelae or indicate improvement in clinical outcomes, respectively. In addition, recovering stroke patients had significant variability in patterns of newly developed neuronal pathways after injury to connected areas of the brain. These findings suggest that the brain attempts to reestablish neuronal connections (plasticity) and that the way in which the brain "heals" may be highly individualized [20]. This technique would have important implications for studies of cCCD including allowing additional data collection from the more chronic phase of injury. Extrapolations of our data would also suggest that immediate changes in resting-state functional MRI connectivity patterns after brain injury may correspond to diaschisis, whereas longitudinal evolution of those may indicate trends and mechanisms similar to those shown by our research.

We recognize that our study has several limitations. Some of those are inherent to the particularities and requirements (1.5 T instead of 3 T imaging, the use of a circular polarized head coil instead of technologically more advanced phase array coils, sometimes incomplete coverage of the cerebellum with DSC perfusion MRI, etc.) of the clinical trial our patients were recruited from, but at the same time, those also assured consistencies in the ways data were collected throughout the entire study period, hence "technically" our retrospective study benefited from many of the merits of a prospectively design research. Also, since no pre-operative DSC perfusion MRI and DTI data were available in our patients, it is unknown if the supratentorial neoplastic processes had already altered the functional characteristics of the cerebellum prior to surgery (possibly implying that our first post-operative studies may not be considered to be true "baselines") and if yes, to what extent. To circumvent this problem, we elected to use an asymmetry index, but also assumed that the other cerebellar hemisphere was "normal."

We acknowledge that the relatively small size of our cohort may be the most significant limitation, and this is certainly the most likely explanation for the relatively significant standard errors in Fig. 2. Since the clinical trial from which our patients were recruited was closed by the time we decided to conduct our research, it was not possible to increase the number of patients, without the risk to introduce new potential confounders. That said, we believe that the remarkably different magnitudes and trends of the observed perfusion and DTI metric changes within cGM and cWM, respectively, validate the robustness not only of our segmentation technique but also the appropriateness of the DSC perfusion MRI and DTI techniques employed in our research and, most importantly, strongly suggest that cerebro-cerebellar diaschisis induces profound, distinctly different and temporally evolving structural and functional changes in cerebellum.

One of the other possible limitations of our study is the age of the patients (children and young adults). Although young age may favor brain plasticity, it is unclear whether age has any effect on the dynamics and prognosis of diaschisis-related pathophysiological, and ultimately, functional changes in brain. This may require further prospective studies. Similarly, we do not know whether or not anti-EGFR therapy, which all of our patients received during the course of care in our institution, has any effect on the magnitude and time course of diaschisis-related hemodynamic changes, because to the best of our knowledge, no data is available in the literature about the possible effect of anti-EGFR agents on normal cerebellar vessels and cerebellar blood circulation. Lastly, although quite unlikely, it is unknown whether radiation therapy delivered to the primary tumor site in the supratentorial compartment has any modulating effect on cerebro-cerebellar functional connectivity and, hence, on the longitudinal evolution of cCCD-related perfusion or diffusion changes in cerebellum.

For all of these reasons, we consider our data "preliminary" to some extent, but hope that our results will trigger further investigations addressing these and other, yet poorly understood, issues.

Conclusion

We endorse the notion that hemodynamic alterations in cGM represent the primary diaschisis phenomena and we propose

that those changes may be reversible. This, however, does not necessarily indicate total normalization of function, because myelin changes, which are likely secondary to extended and persistent underuse, seem to be irreversible. This observation suggests that effective connectivity along the afferent cerebellar pathway may not be reestablished, at least not within the first couple of years after the onset of diaschisis. Although the clinical effect of cCCD is not completely understood, we believe that it is important to investigate the dynamics of underlying pathophysiologic processes to improve our understanding of this apparently uniform response mechanism to remote brain injury. These processes would seem to have implications in other, clinically better-defined, diaschisis-related syndromes, such as cerebellar mutism in postoperative posterior fossa syndrome, and in various, possibly under-recognized "post-injury" functional disorders of the brain. Given our unique patient population and their postsurgical rather than ischemic insult, longitudinal improvement in hemodynamic parameters should be further investigated to ensure its reproducibility in the more-investigated adult ischemic patient population.

Acknowledgments The authors thank Cherise M. Guess for reviewing and editing the manuscript.

Conflict of Interest AB received partial financial support for this research from OSI Pharmaceuticals and Genentech ZP, CP, YL, MS, AB, and RJO received partial support from the US National Institutes of Health Cancer Center Support (CORE) Grant P30 CA21765 and the American Lebanese Syrian Associated Charities (ALSAC) while conducting this research.

The other authors declare no conflict of interest with regard to the subject matter presented in this manuscript.

References

1. Shih WJ, Huang WS, Milan PP. F-18 FDG PET demonstrates crossed cerebellar diaschisis 20 years after stroke. Clin Nucl Med. 2006;31(5):259–61.
2. Kajimoto K, Oku N, Kimura Y, Kato H, Tanaka MR, Kanai Y, et al. Crossed cerebellar diaschisis: a positron emission tomography study with L-[methyl-11C]methionine and 2-deoxy-2-[18F]fluoro-D-glucose. Ann Nucl Med. 2007;21(2):109–13.
3. Krishnananthan R, Minoshima S, Lewis D. Tc-99 m ECD neuro-SPECT and diffusion weighted MRI in the detection of the anatomical extent of subacute stroke: a cautionary note regarding reperfusion hyperemia. Clin Nucl Med. 2007;32(9):700–2.
4. Yamada H, Koshimoto Y, Sadato N, Kawashima Y, Tanaka M, Tsuchida C, et al. Crossed cerebellar diaschisis: assessment with dynamic susceptibility contrast MR imaging. Radiology. 1999;210(2):558–62.
5. Kim J, Lee SK, Lee JD, Kim YW, Kim DI. Decreased fractional anisotropy of middle cerebellar peduncle in crossed cerebellar diaschisis: diffusion-tensor imaging-positron-emission tomography correlation study. AJNR Am J Neuroradiol. 2005;26(9):2224–8.
6. Lin DD, Kleinman JT, Wityk RJ, Gottesman RF, Hillis AE, Lee AW, et al. Crossed cerebellar diaschisis in acute stroke detected by dynamic susceptibility contrast MR perfusion imaging. AJNR Am J Neuroradiol. 2009;30(4):710–5.
7. Team RDC. A language and environment for statistical computing. Vienna: R Foundation for Statistical Computing; 2011.
8. Brunberg JA, Frey KA, Horton JA, Kuhl DE. Crossed cerebellar diaschisis: occurrence and resolution demonstrated with PET during carotid temporary balloon occlusion. AJNR Am J Neuroradiol. 1992;13(1):58–61.
9. Reese TG, Heid O, Weisskoff RM, Wedeen VJ. Reduction of eddy-current-induced distortion in diffusion MRI using a twice-refocused spin echo. Magn Reson Med. 2003;49(1):177–82.
10. Ashburner J, Friston KJ. Voxel-based morphometry—the methods. Neuroimage. 2000;11(6 Pt 1):805–21.
11. Miller NG, Reddick WE, Kocak M, Glass JO, Lobel U, Morris B, et al. Cerebellocerebral diaschisis is the likely mechanism of postsurgical posterior fossa syndrome in pediatric patients with midline cerebellar tumors. AJNR Am J Neuroradiol. 2010;31(2):288–94.
12. Di Costanzo A, Trojsi F, Giannatempo GM, Vuolo L, Popolizio T, Catapano D, et al. Spectroscopic, diffusion and perfusion magnetic resonance imaging at 3.0 Tesla in the delineation of glioblastomas: preliminary results. J Exp Clin Cancer Res. 2006;25(3):383–90.
13. Fox RJ, Sakaie K, Lee JC, Debbins JP, Liu Y, Arnold DL, et al. A validation study of multicenter diffusion tensor imaging: reliability of fractional anisotropy and diffusivity values. AJNR Am J Neuroradiol. 2012;72(2):89–96.
14. Sobesky J, Thiel A, Ghaemi M, Hilker RH, Rudolf J, Jacobs AH, et al. Crossed cerebellar diaschisis in acute human stroke: a PET study of serial changes and response to supratentorial reperfusion. J Cereb Blood Flow Metab. 2005;25(12):1685–91.
15. Flint AC, Naley MC, Wright CB. Ataxic hemiparesis from strategic frontal white matter infarction with crossed cerebellar diaschisis. Stroke. 2006;37(1):e1–2.
16. Gorman MJ, Dafer R, Levine SR. Ataxic hemiparesis: critical appraisal of a lacunar syndrome. Stroke. 1998;29(12):2549–55.
17. Szilagyi G, Vas A, Kerenyi L, Nagy Z, Csiba L, Gulyas B. Correlation between crossed cerebellar diaschisis and clinical neurological scales. Acta Neurol Scand. 2012;125:373–81.
18. Goldsberry G, Mitra D, MacDonald D, Patay Z. Accelerated myelination with motor system involvement in a neonate with immediate postnatal onset of seizures and hemimegalencephaly. Epilepsy Behav. 2011;22(2):391–4.
19. Park CH, Chang WH, Ohn SH, Kim ST, Bang OY, Pascual-Leone A, et al. Longitudinal changes of resting-state functional connectivity during motor recovery after stroke. Stroke. 2011;42(5):1357–62.
20. Inman CS, James GA, Hamann S, Rajendra JK, Pagnoni G, Butler AJ. Altered resting-state effective connectivity of fronto-parietal motor control systems on the primary motor network following stroke. Neuroimage. 2012;59(1):227–37.